Journal of Environmental Chemical Engineering 12 (2024) 112131

Contents lists available at ScienceDirect

Journal of Environmental Chemical Engineering

journal homepage: www.elsevier.com/locate/jece

Control of chlorite and chlorate in drinking water using surfactant-modified activated carbon

Gabriel Sanchez-Cano [a,b,c], Pablo Cristobal-Cueto [b], Paula Nuño-Ortega [b], Lydia Sáez [a], Antonio Lastra [a], Sara Rojas [d,b,*], Patricia Horcajada [b,**]

[a] R&D&I Department, Canal de Isabel II S.A., M.P., Square of Descubridor Diego de Ordás 3, 28003 Madrid, Spain
[b] Advanced Porous Materials Unit, IMDEA Energy Institute, Av. Ramón de la Sagra 3, 28935 Móstoles, Madrid, Spain
[c] Chemical and Environmental Engineering Group, University of Rey Juan Carlos, Tulipán Street s/n, 28933 Móstoles, Madrid, Spain
[d] Inorganic Chemistry Department, Faculty of Science, University of Granada, Av. Fuentenueva s/n, 18071 Granada, Spain

ARTICLE INFO

Editor: Stefanos Giannakis

Keywords:
Activated carbon
Drinking water
Purification
Disinfection by-products
Chlorates
Chlorites

ABSTRACT

Disinfection of drinking water is a fundamental step towards the protection of public health. Particularly, chlorine dioxide is one of the most important disinfection methods applied in public water systems. However, some unwanted and potentially toxic by-products (chlorite-ClO_2^- and chlorate-ClO_3^-) can be generated during this process. Thus, the European Union (EU) has recently set a permissible maximum concentration of 0.25 mg·L^{-1} for both ClO_2^- and ClO_3^- in the water intended for human consumption. Nevertheless, the existent strategies proposed for the elimination of these oxyanions present important limitations for their large-scale application. Here, we propose the ClO_2^- and ClO_3^- adsorption by two granulated activated carbons modified with five different alkyl quaternary ammonium-based surfactants, exhibiting a large affinity for inorganic anions. A granulated activated carbon modified with hexadecylpyridinium chloride monohydrate (CPC@CAG1) was selected as the most efficient adsorbent, achieving an excellent oxyanions removal ($\geq$99 and 80 $\pm$ 0.5% of ClO_2^- and ClO_3^- in only 2 h, respectively). Finally, the ClO_2^- and ClO_3^- elimination was evaluated using a continuous flow under realistic conditions (drinking water from a real treatment plant and 12 min empty bed contact time (EBCT)), reaching a very high oxyanions removal efficacy for 4 cycles of 160 h-each, thus envisioning the future real application of this adsorbent in water disinfection treatments.

1. Introduction

Disinfecting water is the most common process used in drinking water treatment plants (DWTPs), which mainly aims to oxidize organic matter and deactivate harmful bacteria, viruses and other pathogens [1,2]. Among disinfection methods, chlorination (*i.e.,* Cl_2, NaClO) and/or chlorine dioxide (ClO_2) are widely applied because of their outstanding oxidizing power (99.99% bacteria and viruses can be eliminated with only 6–70 mg·L^{-1}·min^{-1}) [3]. However, these processes can further generate unwanted and potentially toxic disinfection by-products (*e.g.,* trihalomethanes (THMs) or haloacetic acids (HAAs)) from the reaction of chlorine with organic matter, or chlorite (ClO_2^-) and chlorate (ClO_3^-) through disproportionation of disinfecting reagents [4,5]. Despite the low toxicity of these compounds (*i.e.,* ClO_3^- oral median lethal dose in rats (LD_{50}) > 3861 mg·Kg^{-1} or in humans 50 mg·kg^{-1}), recent studies correlated their presence in drinking water with chronic illnesses [6]. Indeed, after long-term exposure, ClO_2^- and ClO_3^- may cause methemoglobin, associated with the oxidative stress of the interconversion reaction of ClO_2^-, ClO_3^-, and chloride in the gut [6]. Further, ClO_3^- can act as a competitive inhibitor of iodine uptake in the thyroid glands, resulting in hormonal disorders and related illnesses (*e.g.,* hypothyroidism) [6,7].

In view of the above, the European Union (EU) has recently proposed a permissible maximum concentration of 0.25 mg·L^{-1} for both ClO_2^- and ClO_3 in the water intended for human consumption (Directive 2020/2184) [8]. Particularly, the elimination of ClO_3^- *via* degradation is a difficult task due to its high stability. Although the reduction of ClO_3^- is thermodynamically favorable ($E^0(ClO_3^-/Cl_2)$ = 1.468 V under acidic conditions), this reaction is extremely complex as it presents a very slow kinetics and occurs at low pH values, far from those found in drinking water (pH = 6.5 - 8.5) [9]. On the other hand, ClO_2^- negatively affects the

* Corresponding author at: Inorganic Chemistry Department, Faculty of Science, University of Granada, Av. Fuentenueva s/n, 18071 Granada, Spain.
** Corresponding author.
E-mail addresses: srojas@ugr.es (S. Rojas), patricia.horcajada@imdea.org (P. Horcajada).

https://doi.org/10.1016/j.jece.2024.112131
Received 2 October 2023; Received in revised form 28 December 2023; Accepted 1 February 2024
Available online 3 February 2024

post-UV/chlorine process due to its strong radical scavenging effect, also enhancing the formation of ClO_3^- [10,11]. Until now, different approaches have been proposed to eliminate ClO_3^- and ClO_2^- from drinking water: adsorption (based on membranes, ion-exchange resins), reverse osmosis, chemical reaction (heterogeneous catalysis) or biological processes [12,13]. For instance, Fe(II) compounds are able to reduce the ClO_2^- and ClO_3^- content in water up to 99 and 55%, respectively [14]. The bioelectrochemical process using *Dechloromonas agitate CKB* bacteria has also demonstrated to transform up to 5.7 g of $ClO_3^-{\cdot}m^{-3}{\cdot}day^{-1}$ to Cl^- [15–18]. Further, heterogenous catalysts based on precious metals (*e.g.*, Pt, Pd) remove up to 99% of ClO_3^- through hydrogenation reaction [19]. Although promising technologies for the chlorination by-products elimination, their large-scale application is strongly limited by the complex implementation and maintenance, high cost and/or poor durability.

Porous materials constitute a relevant alternative since they combine a high porosity and chemical stability with a low operation cost, easy implementation, and large techno-economic feasibility. In particular, activated carbon (AC) filtration is one of the most frequent processes used in DWTPs (*e.g.,* pre-oxidation, disinfecting stages) to adsorb organic species, per- and polyfluoroalkyl substances (PFASs), free or residual Cl_2 and, in general, compounds affecting odor and taste [20]. Further, ACs have demonstrated their ability to efficiently adsorb several oxyanions, such as ClO_4^-, NO_3^-, or PO_4^{3-}, among others.[21,22] However, the ClO_2^- and ClO_3^- elimination using ACs have been scarcely studied [5]. In fact, only two reports, dating from 1983 and 1994, have proposed granulated active carbon (GAC) for the elimination of ClO_2^- [23,24]. The first one reported the combined elimination of ClO_2^- (80 mg of $ClO_2^-{\cdot}g^{-1}$ of GAC) and vanillic acid or indan under static conditions [5, 23], and the second one investigated the removal of ClO_2^- and ClO_3^- under water continuous flow, reaching rates of 162 mg of $ClO_2^-{\cdot}g^{-1}$ (2.3 $mg{\cdot}L^{-1}$ influent) and 4.9 mg $ClO_3^-{\cdot}g^{-1}$ (5.0 $mg{\cdot}L^{-1}$ influent). However, the empty bed contact times (EBCT) employed here were much shorter than the ones normally used in practice (0.35 & 0.18 min *vs.* 5–15 min).

In a further step to improve its oxyanions sorption properties, ACs can be combined with other species. Particularly, the modification of GACs with alkyl quaternary ammonium-based surfactants, with large affinity for low hydration energy inorganic anions, has been reported for the efficient ion exchange of different species (amino acids, BrO_3^-, NO_3^-, or ClO_4^-) [25]. Compared with previously reported ACs modifications in the adsorption of anionic species in water (such citric acid, sulfuric acid or nitric acid modified AC in the adsorption of F^-) [26–28], cationic surfactants is preferred in water treatment since their hydrophobic character makes them useful in the elimination of non-polar contaminants (*e.g.,* dissolved organic matter) [29]. However, up to our knowledge, this strategy has never been proposed for the ClO_2^- and ClO_3^- adsorption. This is probably due to the low reactivity and affinity of these oxyanions to AC in comparison with ClO_4^-, a more reactive specie mainly adsorbed by electrostatic attraction and hydrogen bonding to oxygen containing groups of ACs. The challenge here is to efficiently adsorb the less reactive ClO_2^- and ClO_3^- (*e.g.,* through ion exchange, electrostatic interactions or surface complexation) over the large panel of ions present in drinking water [30–32].

Thus, in this study we originally propose to eliminate ClO_2^- and ClO_3^- from real disinfected water samples using cationic surfactant-modified GACs. Initially, the modification of two different GACs with various cationic surfactants containing quaternary ammonium groups was carried out, selecting the best performing material in terms of ClO_2^- and ClO_3^- removal upon a fast screening under static conditions. Then, the influence of the initial anions' concentration on the adsorption kinetics of ClO_2^- and ClO_3^- was assessed in a detailed study. Finally, in view of the practical use of the selected material, the ClO_2^- and ClO_3^- removal was evaluated using a continuous water flow under realistic EBCT conditions (12 min), compatible with DWTPs operation, and also considering the potential regeneration under continuous conditions.

2. Materials and methods

2.1. Materials

All reactants and solvents were commercially obtained from Sharlau (granulated charcoal activated carbon, (GAC1), Sigma Aldrich (Norit® RX3 Extra (NRX3), and H_2SO_4 (95–97%)), hexadecylpyridinium chloride monohydrate (also known as CPC), hexadecyltrimethylammonium chloride (CTAC, ≥97%), myristyltrimethylammonium bromide (MTAB, ≥99%), decyltrimethylammonium bromide (DTAB, ≥98%), and sodium carbonate (Na_2CO_3) solution (72 mM in water for Metrosep A Supp 7), and Merck (hexadecyltrimethylammonium bromide (CTAB, ≥ 97%)), and used without further purification. Drinking water samples were supplied by Canal Isabel II S.A., M.P. (Spain).

2.2. Preparation of quaternary ammonium surfactant-modified GACs

For the efficient and practical removal of ClO_3^- and ClO_2^- from drinking water, shaped GAC materials were selected over powdered ACs, since they present some advantages for their implementation in continuous flow devices, such as an easy fixed-bed column design and routine maintenance, a low leaching of the solid, and the prevention of high back pressure. The functionalized GACs were prepared following a previously reported method [33]. Briefly, 1 mmol of surfactant (0.364, 0.358, 0.320, 0.336 and 0.280 g of CTAB, CPC, CTAC, MTAB and DTAB, respectively) was dissolved in 100 mL of Milli-Q water under stirring for 15 min. Then, 125 mmol (1.5 g) of GAC (GAC1 or NRX3, molar ratio surfactant:GAC 1:125) were added to the previously prepared solution at room temperature for 5 h under strong magnetic stirring. Surfactant-modified carbons (Surfactant@GAC) were collected by filtration under vacuum and washed with 300 mL of Milli-Q water in order to eliminate the excess of surfactant. The modified materials were dried at 60 °C for 24 h.

2.3. Physicochemical characterization and water analysis

Physicochemical characterization: X-ray powder diffraction (XRPD) patterns were collected from 5 to 35° (2θ) using a step size of 0.013° and a scanning speed of 0.013 s^{-1} by a conventional PANalytical Empyrean powder diffractometer (PANalytical Lelyweg, Netherlands, $\theta - 2\theta$ equipped with λCu $K_{\alpha1}$ and $K_{\alpha2}$ radiation (λ = 1.54051 and 1.54443 Å), equipped with PIXcel3D detector, operating at 45 kV and 40 mA. Thermogravimetric analyses (TGA) were performed on a SDT Q-600 thermobalance (TA Instruments, New Castle, USA) under air flow (100 $mL{\cdot}min^{-1}$) from room temperature to 750 °C with heating profile of 5 °C·min^{-1}. Fourier transform infrared (FTIR) spectroscopic analyses were collected in a Nicolet 6700 (Thermo Scientific, USA) infrared spectrometer in an attenuated total reflectance (ATR) mode by averaging 64 scans at a maximum resolution of 4 cm^{-1} in the 4000–500 cm^{-1} wavenumber range. Nitrogen sorption isotherms were obtained at 77 K using a Micromeritics ASAP2020 surface area and porosity analyzer. Prior to the experiments, ACs and Surfactant@ACs were degassed at 200 and 100 °C for 16 h under vacuum, respectively. The Brunauer-Emmett-Teller (BET) equation was used to calculate the specific surface area in the relative pressure interval $p/p_0 = 0.01–0.3$ (being p_0 the saturation pressure). Pore size distribution and pore volume were estimated by the Horvath-Kawazoe (HK) method using a sphere geometry model (p/p_0 = 0–0.98). The external surface, microporosity area and volume were determined by the t-plot method (p/p_0 from 0.3–0.6). Elemental analyses (EA) were performed in a Flash 2000 analyzer (Thermo Scientific). The aqueous CPC detection was performed by UV–vis spectroscopy (λ_{max} = 259 nm) in a Perkin® Lambda 1050 UV/Vis/NIR equipment (Perkin Elmer, Waltham, MA, USA).

Ionic Chromatography (IC): The anions content in water was analyzed using a 930 Compact IC Flex (Metrohm Hispania, Spain), equipped with a 919 IC autosampler plus, a high-pressure isocratic pump with double-

piston system in series (flow rate 0.001–5 mL·min^{-1}), an IC conductivity detector (operating ranges from 0 to 10,000 μS·cm^{-1}), column oven (0 to 80 °C), and STREAM sequential suppressor (suppressor treatment with reused eluent after measuring), consisting of a chemical suppressor MSM II (Metrohm suppressor module) and CO_2 suppressor MCS (Metrohm CO_2 suppressor) with a vacuum microchamber. The STREAM sequential suppressor was regenerated with a 500 mM H_2SO_4 solution in fresh Milli-Q water, 15% v/v acetone and 100 mM of oxalic acid solution in fresh Milli-Q water, equipped with an 807 Deosing. The eluent consisted of a 3.6 mM Na_2CO_3 solution in fresh Milli-Q water. Samples were retained in a Metrosep A Supp 7 column (5 μm, 250 nm x 4 mm, Metrohm Hispania, Spain), consisting of a resin of polyvinyl alcohol with quaternary ammonium group. The column was also equipped with a Metrosep A Supp 5 Guard pre-column (5 μm, 5 mm x 4 mm, Metrohm Hispania, Spain) and a Metrosep A Supp 16 S-Guard post-column (4.6 μm, 5 mm x 4 mm, Metrohm Hispania, Spain) formed by polystyrene/divinyl benzene copolymer with quaternary ammonium group. Analyses were performed using a flow rate of 0.7 mL·min^{-1}, at 45 ºC and with an injection volume of 100 μL. The retention time for F^-, ClO_2^-, Cl^-, NO_2^-, Br^-, ClO_3^-, NO_3^-, and SO_4^{2-} were 6.94, 9.51, 11.07, 13.52, 16,52, 17.96, 19.74, and 30.58 min, respectively (Supporting information-SI-, Fig. S1 and Table S1).

2.4. Screening of chlorite and chlorate adsorption

ClO_2^- and ClO_3^- adsorption studies were performed by suspending 5 mg of ACs (GAC1 or NRX3) or their surfactant modified version (Surfactant@GAC, Surfactant = CTAB, CPC, CTAC, DTAB or MTAB), previously grinded to avoid interparticle diffusion mechanism, in 5 mL of drinking water, using a high initial concentration of ClO_2^- and ClO_3^- of 0.3 and 3.3 mg·L^{-1}, respectively. Note that the used oxyanions concentrations are in the range or higher than the maximum permissible concentration 0.25 mg·L^{-1} set by the new directive of the EU to evaluate the influence of oxyanions under extreme high concentration conditions [8]. After been stirred (400 rpm) for 2 h at room temperature, the suspensions were filtered under vacuum and the liquid was analyzed by IC.

2.5. Kinetic adsorption experiments: concentration influence

The kinetic adsorption experiments were performed by suspending 10 mg of material (GAC or Surfactant@GAC), previously grinded to avoid interparticle diffusion effect, in 10 mL of drinking water for 30 min under stirring (400 rpm). Two different initial concentrations of ClO_2^- and ClO_3^- were tested: low concentration at 0.1 and 0.25 mg·L^{-1}, and high concentration at 0.3 and 3.3 mg·L^{-1} of ClO_2^- and ClO_3^-, respectively. The concentration of ClO_2^- and ClO_3^- was selected according to the anion concentration found in drinking water and the new regulations [9,23]. When necessary, real water samples were doped with ClO_2^- and ClO_3^-. At certain intervals of time (1, 2, 3, 4, 5, 15 and 30 min), an aliquot of 1 mL was collected by filtration and analyzed by IC. All these experiments were performed at least triplet.

2.6. Continuous flow adsorption and adsorbent regeneration

2.6.1. Continuous flow adsorption

A fixed bed column made of plastic tube (internal diameter Ø = 1.6 cm, and column length = 7.1 cm and bed length = 2.5 cm) equipped with a nylon filter (pore = 0.22 μm) located in the effluent outlet was used as column. The GAC or Surfactant@GAC (2 g) was placed inside the column and water was passed downstream. The dead volume inside the column was negligible. The oxyanions adsorption was carried out using a Shenchen LabN1-II peristaltic pump system with a continuous flow of 0.42 mL·min^{-1} (equivalent to a flux of 0.12 m^3·h^{-1}·m^{-2} and an EBCT of 12 min, typically used in DWTPs). Experiments were performed using low (0.1 and 0.25 mg·L^{-1}) and high concentration (0.3 and 3.3 mg·L^{-1}) of ClO_2^- and ClO_3^-, respectively. Aliquots of 2 mL were collected at different time intervals and the concentration of the different ionic species was determine by IC. All continuous flow experiments were developed by triplicate.

2.6.2. Regeneration of the adsorbent under static conditions

The regeneration initial tests were carried out under magnetic stirring (400 rpm) at room temperature and using 10 mg of CPC@GAC1 material. The activated carbon was suspended in different aqueous solutions of low (6.3 mM) and high concentration (12.6 mM) of NaCl and NaOH, respectively, which corresponds to 2 and 4-fold the concentration of Cl^- present in the surfactant. At certain intervals of time (0.25, 0.5, 1.5, 2, 4, 6, 8, 24, 32, and 48 h), an aliquot of 1 mL was collected by filtration using a syringe filter of 0.22 μm and analyzed by IC.

2.6.3. Continuous flow regeneration and Recycles

After each continuous flow adsorption test (total time = 160 h), the CPC@GAC1 column was regenerated using a 12.6 mM of NaCl solution (total time = 56 h) and the same set up used in the continuous flow adsorption experiments (internal diameter Ø = 1.6 cm, column length = 7.1 cm, bed length = 2.5 cm, continuous flow of 0.12 m^3·h^{-1}·m^{-2} and EBCT of 12 min). Finally, the recycling experiments were carried out using a drinking water with oxyanions concentration of 0.1 and 0.25 mg·L^{-1} for ClO_2^- and ClO_3^-, respectively. The concentration of oxyanions in the effluent was analyzed by IC at different time intervals. The experiments were carried out by triplicate.

3. Results and discussion

Two commercially available GACs were chosen, GAC1 and NRX3, exhibiting large surfaces (1400 and 1220 m^2·g^{-1}), low cost (0.17 and 0.23 €·g^{-1}), and pellet distribution variability (length: 4 and 9 mm, Ø: 1 and 3 mm), respectively [34,35]. Then, in an attempt to boost the oxyanions adsorption, their surface was modified using five quaternary ammonium surfactants with different properties (*i.e.,* chain length, polar head size, counter-anion; CTAB, CTAC, CPC, MTAB and DTAB; see

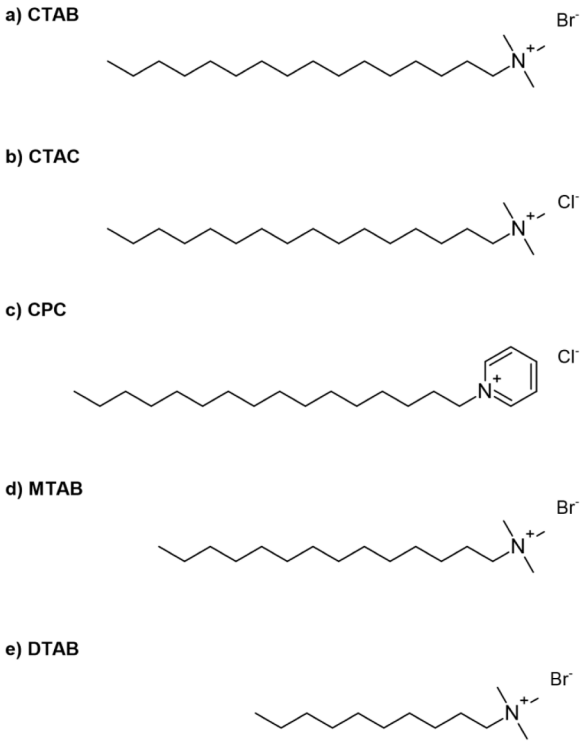

Fig. 1. Chemical structure of cationic surfactant based on ammonium quaternary a) CTAB, b) CPC, c) CTAC, d) MTAB, and e) DTAB.

Fig. 1) using a simple and efficient green aqueous impregnation method (see Section 2.2 in Materials and Methods). The amount of associated surfactant, determined by elemental analysis and thermogravimetric analysis (TGA; see Table 1, and Supporting information-SI, Fig. S2 & Table S3), reached 0.27 ± 0.07, 0.33 ± 0.15, 0.40 ± 0.01, 0.48 ± 0.14, and 0.53 ± 0.08 mmol of surfactant·g^{-1} GAC1, and 0.22 ± 0.06, 0.34 ± 0.23, 0.26 ± 0.08, 0.29 ± 0.12, and 0.41 ± 0.12 mmol of surfactant·g^{-1} NRX3 for CTAB, CTAC, CPC, MTAB and DTAB, respectively. A similar trend can be observed for both GACs: a higher surfactant grafting when using short alkyl chain surfactants (MTAB with C14 and DTAB with C10 chain) than using long alkyl chain ones (CTAB, CPC and CTAC with C16 chain). When comparing surfactants with identical chain length but different functional groups, like CTAB and CPC with trimethylammonium and pyridinium groups, respectively, differences on the surfactant association are observed between GACs, with a higher CPC surfactant content than CTAB in GAC1 (0.27 ± 0.07 *vs* 0.40 ± 0.01 mmol·g^{-1}, respectively), and the opposite trend in NRX3 (0.22 ± 0.06 and 0.26 ± 0.08 mmol·g^{-1} for CTAB and CPC, respectively). Besides, identical alkyl chain surfactants with different counter-ion nature (Cl^- and Br^-) show higher impregnation rates when using Cl^- (CTAC; 0.33 ± 0.15 and 0.34 ± 0.23 mmol of surfactant·g^{-1} for GAC1 and NXR3, respectively) than Br^- (CTAB; 0.27 ± 0.07 and 0.22 ± 0.06 mmol of surfactant·g^{-1} for GAC1 and NXR3, respectively). This effect is probably related with the different ionic radius of Cl^- and Br^- (1.64 *vs.* 1.80 Å, respectively), which might promote the formation of spherical *vs.* cylindrical micelles, respectively [36,37].

The successful surfactant modification was demonstrated through N_2 sorption isotherms measured at 77 K, since the accessible porosity of the GAC was significantly reduced (SI, Figs. S3). Despite this reduction, all solids kept an important residual porosity after the surfactant grafting (between 55–64% and 76–91% for Surfactant@GAC1 and Surfactant@NRX3, respectively). Specifically, starting GAC1 and NRX3 materials are mostly microporous (~1.5 nm). Thus, the surfactant molecules or even their micelles (ranging from 1 to 5 nm) could be located in the inner porosity and/or on the outer surface of the AC particles [38,39]. To address this issue, corrected surface area values were estimated by subtracting the surfactant weight (Table 1). Upon correction, no significant variation of the surface area is observed between the CTAC-, MTAB- and DTAB-surfactant@NRX3 and the pristine NRX3 (1155, 1180 and 1040 *vs.* 1220 $m^2 \cdot g^{-1}$, respectively), suggesting the preferential location of the surfactant on the outer surface of the AC particles. In contrast, surface variations are evidenced for all the Surfactant@GAC1 materials (ranging from 325 and 480 $m^2 \cdot g^{-1}$) and for the CTAB and CPC surfactants with the NR3X (~275 $m^2 \cdot g^{-1}$). Unexpectedly, using the largest CTAB and CTAC surfactants, and therefore, less probable to diffuse within the porosity, the accessible porosity values were not recovered. However, CTAB, CTAC and CPC show smaller micelle sizes (SI, Table S2) than other surfactants. These results could be related to hydrophobic interactions or micelle aggregates formation. In fact, while the GAC modification with CTAB, CPC, CTAC and MTAB was carried out using a surfactant concentration higher than the surfactant critical micelle concentration (CMC; 0.9, 0.8, 1.1 and 3.6 mmol·L^{-1}, respectively), the functionalization with DTAB was done below the CMC (15.3 mmol·L^{-1}) [33,40]. Although this is a complex matter with no enough data to conclude, the formation of micelles or larger aggregates of the surfactant could affect the association to the GAC in different manners: i) larger sizes might hamper the diffusion through the pores, ii) hydrophobic interactions could benefit the incorporation, and/or iii) formation of aggregates could hamper the accessibility of N_2 into the porosity [33].

To shed some light on the nature of the interactions between GACs and surfactants, Fourier transform infrared (FTIR) spectroscopy was also performed (SI, Section S3). Compared with the free surfactants, spectra of the Surfactant@GAC materials exhibit additional bands at 2915 and 2847 cm^{-1}, characteristic of alkyl chain stretching bands [41]. In this regard, there is a shift in the position of those bands for all functionalized ACs (SI, Table S4), suggesting the formation of interactions between the surfactants and the ACs. One could speculate the formation of van der Waals interactions, hydrogen bonds between the N^+ group from the surfactant and the carboxylic, phenolic or carbonyl groups potentially present in the AC, and/or π-π interactions in the case of the CPC surfactant between its pyridinium ring and the AC surface, as described in previous studies [42,43].

Finally, the X-ray powder diffraction (XRPD) patterns of the obtained Surfactant@GACs confirmed the amorphous structure of the AC (SI, Fig. S5), maintaining diffraction of some peaks at around 23° 2θ, corresponding to the basal plane of graphitic structure in pristine carbons without changing the amorphous structure carbons during the impregnation method [44,45].

3.1. Screening of the chlorite and chlorate removal

For the screening of the ClO_2^- and ClO_3^- adsorption capacity, modified GACs were suspended for 2 h in tap water solutions doped with high oxyanions concentration (0.3 and 3.3 mg·L^{-1} of ClO_2^- and ClO_3^-, respectively) in order to accelerate the material saturation. It should be noted that these dangerous concentration values have been previously detected in DWTPs around the world, such as in drinking water from different regions of Chile [46]. All Surfactant@GAC materials showed outstanding results in the ClO_2^- and ClO_3^- elimination. Interestingly, the functionalization positively influences the oxyanions' elimination, improving the ClO_3^- removal capacity of the bare GAC (between 2.2 to 2.4-fold and 1.5 to 1.6-fold for Surfactant@GAC1 and Surfactant@NRX3, respectively, Fig. 2). The amount of eliminated ClO_3^-

Table 1
Surfactant content (mmol of surfactant per g of GAC), and textural properties (BET surface-S_{BET}, pore volume-V_p, particle size-P_S) of the two tested GACs before and after the surfactant modification.

Surfactant/GAC	GAC1				NRX3			
	mmol·g^{-1}	S_{BET} ($m^2 \cdot g^{-1}$)	V_p ($cm^3 \cdot g^{-1}$)	P_s (Å)	mmol·g^{-1}	S_{BET} ($m^2 \cdot g^{-1}$)	V_p ($cm^3 \cdot g^{-1}$)	P_s (Å)
Pristine GAC	-	1400	0.64	14.5	-	1220	0.57	13.7
CTAB	0.27 ± 0.07	880 (980)[a]	0.42	14.4	0.22 ± 0.06	935 (1005)[a]	0.42	12.1
CTAC	0.33 ± 0.15	865 (950)[a]	0.42	14.5	0.34 ± 0.23	1080 (1155)[a]	0.50	12.5
CPC	0.4 ± 0.01	780 (920)[a]	0.38	13.2	0.26 ± 0.08	955 (1040)[a]	0.44	12.9
MTAB	0.48 ± 0.14	885 (1030)[a]	0.42	13.0	0.29 ± 0.12	1180 (1285)[a]	0.58	14.1
DTAB	0.53 ± 0.08	910 (1075)[a]	0.43	12.6	0.41 ± 0.12	1040 (1145)[a]	0.48	12.8

[a] Normalized value by subtracting the surfactant weight.

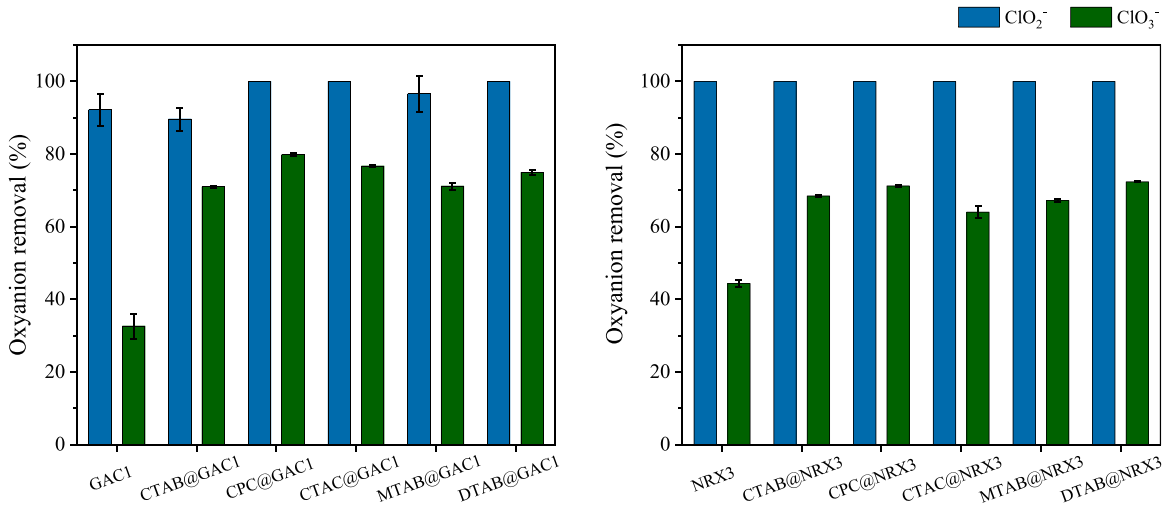

Fig. 2. Removal (%) of chlorites (blue bars) and chlorates (green bars) on original and modified GAC1 (left) and NRX3 (right) with different cationic surfactants. (For interpretation of the references to color in this figure legend, the reader is referred to the web version of this article.)

depends on the nature of the surfactant, and decreases in the following order: CPC (79.9 ± 0.5%) > CTAC (76.7 ± 0.3%) > DTAB (74.9 ± 0.6%) > MTAB (71.2 ± 1.0%) ≈ CTAB (71.0 ± 0.3%) > > bare GAC1 (32.6 ± 3.4%) for GAC1 materials, and DTAB (72.4 ± 0.2%) ≈ CPC (71.2 ± 0.2%) > CTAB (68.5 ± 1.7%) ≈ MTAB (67.2 ± 0.4%) > CTAC (64.0 ± 1.7%) > > bare NRX3 (44.4 ± 1%) for NRX3 samples. These results highlight the efficiency of Surfactant@GAC in the removal of ClO_3^-, eliminating up to 80.0% of the ClO_3^- present in drinking water in only 2 h. Regarding ClO_2^- removal, the tested GACs showed a very good ClO_2^- adsorption capacity, reaching a complete or almost complete elimination regardless the AC or surfactant nature (Fig. 2), and in all cases exceeding the capacities obtained with the pristine ACs.

It should be noted that, in general terms, the Surfactant@GACs with higher accessible porosity were not the more efficient ones in the elimination of oxyanions. For instance, CPC@GAC1, with one of the lowest S_{BET} value (920 $m^2 \cdot g^{-1}$), demonstrated a remarkable elimination capacity of 100 ± 0 and 79.9 ± 0.5% of ClO_2^- and ClO_3^- in only 2 h. On the other hand, the elimination mechanism seems to be driven by Cl^- or Br^- ions exchange processes, as supported by the sharp increase of these anions in the treated water (*i.e.,* from 0.09 ± 0.03 to 24.74 ± 0.05 $mg \cdot L^{-1}$ for Br^- in DTAB@GAC1, and from 14.12 ± 0.13 to 23.65 ± 0.2 $mg \cdot L^{-1}$ for Cl^- in CTAC@GAC1; SI Figs. S6-9). Likewise, other inorganic anions were assessed in the drinking water. While nitrite (NO_2^-) or fluoride (F^-) concentrations were not significantly affected during ClO_2^- and ClO_3^- adsorption processes, nitrate (NO_3^-) and sulphate (SO_4^{2-}) were adsorbed in Surfactant@GAC materials (*i.e.,* from 3.19 ± 0.02 to 1.26 ± 0.04 $mg \cdot L^{-1}$ and from 10.90 ± 0.01 to 7.00 ± 0.1 $mg \cdot L^{-1}$ for NO_3^- and SO_4^{2-} in CPC@GAC1, respectively; SI, Figs. S6-9). Thus, we can confirm that surfactant-modified materials exhibit a high affinity for ClO_2^- and ClO_3^- removal and can complementary eliminate NO_3^- and SO_4^{2-}. The results showed that nitrate, with a similar geometry and charge, is the main competitor of ClO_3^-, achieving total adsorption values from 21.4 to 60.6% and calculated selectivity values from 28.6 to 34.4% in all Surfactant@GACs (SI, Table S5)."

Finally, among the tested materials, the most promising one is the CPC@GAC1, achieving adsorption capacities of 0.24 ± 0 and 2.5 ± 0.02 $mg \cdot g^1$, ClO_2^- and ClO_3^-, respectively (or 100.0 ± 0% and 79.9 ± 0.5%, respectively). Thus, a further step was the analysis of the potential leaching of CPC during oxyanions adsorption process by UV–vis. Results confirmed the absence of free CPC, with a low oral toxicity (oral LD_{50} = 560.3 $mg \cdot kg^{-1}$ in rat) [47], in all water samples (limit of detection = 0.0017 mM), exhibiting the potential of CPC@GAC materials in water treatment.

3.2. Kinetic experiments and influence of oxyanions concentration

At this point, in an attempt to gain further understanding on the involved mechanism and to make this process more efficient for practical uses, a deeper kinetic study was performed using the bare GAC1 and CPC@GAC1 materials by monitoring the oxyanions adsorption as a function of time (<30 min) and concentration (Fig. 3). Two different ClO_2^- and ClO_3^- concentrations were selected: i) a denoted "low concentration" of 0.1 and 0.25 $mg \cdot L^{-1}$, respectively, corresponding to the frequently reported real composition of drinking water [48–50], and ii) a 3 and 13-fold higher concentrated tap water (0.3 and 3.3 $mg \cdot L^{-1}$, respectively; named "high concentration"), similar to the previously used in the screening tests (Section 3.1). The ClO_2^- and ClO_3^- elimination was very fast when using both, pristine and surfactant modified GAC1, reaching the maximum oxyanion removal in only 5 min. In particular, the kinetics could be fitted to the pseudo-second kinetic (PSO) model, which defines the short time performance, involving ion-exchange reaction between adsorbate with active sites on surface material, electrostatic interactions, *etc.*; (Table 2, see SI Section 5 for further details) [51–53]. Note here that GAC1 and CPC@GAC1 were previously grinded and the kinetic studies performed under continuous stirring to exclude/minimize the external diffusion process around the particles. Thus, the adsorption process might be exclusively due to the ion-exchange through the AC surface. Therefore, the ClO_2^- and ClO_3^- adsorption could be explained by the following equation:

$$\frac{dq(t)}{dt} = K_2 \cdot (q_e - q(t))^2 \rightarrow \frac{t}{q_t} = \frac{1}{K_2 \cdot q_e^2} + \frac{t}{q_e} \quad (1)$$

where q_e is the maximum adsorption capacity at the equilibrium ($mg \cdot g^{-1}$), q_t is the adsorption capacity with time ($mg \cdot g^{-1}$), and K_2 is the kinetic constant ($g \cdot mg^{-1} \cdot min^{-1}$).

Except for CPC@GAC1 @ClO_2^- and GAC1 @ClO_3^-, with regression factors (R^2) < 0.99, the rest of oxyanions adsorption processes can be empirically adjusted in the first 5 min (ClO_2^-) and 15 min (ClO_3^-) to a PSO with R^2 > 0.99 (Table 2, Fig. S10). Therefore, it can be concluded that the adsorption process is mainly governed by an ionic-exchange process, predictable by the PSO model where various assumptions are considered (*i.e.,* adsorption at specific sites with no interaction between the adsorbates, and attainment of monolayer coverage on the adsorbent surface yields maximum adsorption) [54]. It should be noted that considering the final application (purification of drinking water), it is imperative to get fast adsorption kinetics in order to achieve more efficient treatments. The initial adsorption rate can be easily compared

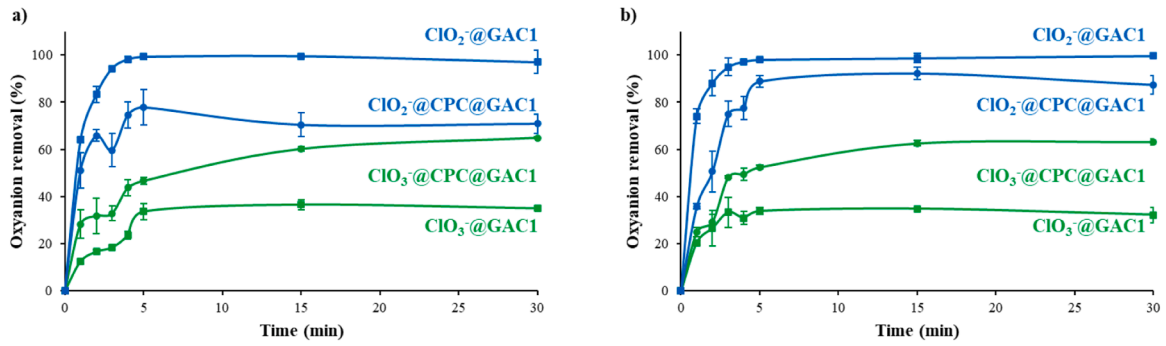

Fig. 3. Chlorite (blue) and chlorate (green) removal at (a) low and (b) high oxyanions concentration using the bare GAC1 (squares) and CPC@GAC1 (circles). (For interpretation of the references to color in this figure legend, the reader is referred to the web version of this article.)

Table 2
K_2 values (g·mg^{-1}·min^{-1}), R^2, and maximum loading capacity (q_e, mg·g^{-1}) obtained in the fitting of the adsorption of ClO_2^- and ClO_3^-in GAC1 and CPC@GAC1 at low and high concentrations using the pseudo-second order (PSO).

	Low concentration		High concentration	
	GAC1	CPC@GAC1	GAC1	CPC@GAC1
ClO_2^-				
K_2	11.46	16.41	8.38	0.85
(R^2)	(0.999)	(0.997)	(0.994)	(0.974)
q_e	0.11	0.08	0.31	0.37
ClO_3^-				
K_2	3.21	3.01	1.01	0.23
(R^2)	(0.988)	(0.994)	(0.999)	(0.993)
q_e	0.10	0.16	1.21	2.19

by estimating the kinetic constants (Table 2), evidencing that the ClO_2^- adsorption is faster (from 3.6 to 8.2-fold) than the ClO_3^- one in both materials. At low oxyanions concentration, similar kinetic constants (K_2) and theoretical maximum (q_e) oxyanions cargo are observed when GAC1 or CPC@GAC1 are used as adsorbent; except for the ClO_2^- adsorption in CPC@GAC1, where the kinetics is 1.4 times faster than the GAC one. At higher concentration, GAC1 faster adsorbs ClO_2^- and ClO_3^- (9.9 and 4.2-fold) than CPC@GAC1. However, the theoretical maximum oxyanions cargo is similar (ClO_2^-) or *ca.* 2 times higher (ClO_3^-) when CPC@GAC1 is used. At this concentration, the q_e obtained values are remarkably higher and the K_2 lower, since in the PSO model a modification of the initial concentration will directly affect the equilibrium, increasing the adsorption capacity and, therefore, slower reaching the equilibrium state and causing a reduction in the equilibrium constant [51,55].

3.3. Real in-continuous flow testing

Taking advantage of the efficient performance of CPC@GAC1 in the ClO_2^- and ClO_3^- adsorption and to further demonstrate the potential practical application of this composite in drinking water treatment, a specific in-continuous flow device based on CPC@GAC1 was developed to work under real drinking water conditions. It is important to mention that the water flow used during the experiments (0.42 mL·min^{-1}, equivalent to *ca.* 0.12 m^3·h^{-1}m^{-2} and a bed contact time of 12 min) is within the range typically used in DWTPs (*i.e.,* 5–15 min) [56]. The selected GAC1 material is already commercialized as granules, which facilitates its implementation in DWTP's avoiding high backpressure. Finally, considering the large variation in influent drinking water concentration (even intra-day), a peristaltic pump was used to control the upward water flow using low (0.1 and 0.25 mg·L^{-1}) and high concentrated tap water solutions (0.3 and 3.3 mg·L^{-1}) of ClO_2^- and ClO_3^-, respectively (SI, Fig. S11).

The breakthrough curve demonstrated that the designed CPC@GAC1 column was able to successfully adsorb up to 90% of the ClO_3^- from drinking water during 3 and 3.7 days, and 80% of ClO_3^- during 4.2 and 5.5 days at high and low oxyanions concentrations waters, respectively (Fig. 4). Regardless the concentration, the time to reach 50% of saturation ($t_{50\%}$) was 6.3 and 6.6 days for high and low oxyanions concentration. These impressive values largely exceed those obtained with the non-functionalized GAC1 (at low concentration with a $t_{50\%}$ less than 1.3 days, 5.6-fold better performing).

Further, ClO_2^- was 100% eliminated in all tested conditions. This is probably due to the reduction from ClO_2^- to Cl^- by oxidation of organic matter with interaction with GAC1, as previously reported [5].

The adsorbent regeneration is a crucial point for its sustainable and economical application. The current methods for the regeneration of ACs include thermal, chemical, microwave, wet oxidation, electrochemical and bioregeneration processes [57]. Here, a simple and economic one-step anionic exchange process was used, evaluating its efficacy by IC using two anions at two different concentrations (6.3 and 12.6 mM of NaCl and NaOH, see Supporting information-SI Fig. S12). High values of released ClO_3^- were achieved when using both treatments at high concentration (24 and 54% for NaCl and NaOH after 8 h, respectively). Then, when the regenerated materials were reutilized in a second oxyanions' adsorption step under continuous flow, their adsorption capacity after the treatment with NaCl was maintained, while for NaOH it was importantly diminished. Therefore, the treatment with NaCl (12.6 mM) was selected for the regeneration of CPC@GAC1 after ClO_2^- and ClO_3^- adsorption. On the other hand, no ClO_2^- was desorbed with any of the regeneration treatments, supporting the hypothesis of its reduction to Cl^- (see above) [5]. Importantly, the absence of surfactant in the effluent of the first regeneration cycle was demonstrated by UV-Vis spectroscopy (limit of detection (LOD) of CPC was estimated to be 0.0017 mM).

Finally, the potential reusability of the adsorbent was tested by successive adsorption (total time of the process = 160 h) and desorption (total time of the process = 56 h) cycles under continuous flow. After 4 cycles, CPC@GAC1 was able to eliminate 100 and 50% of ClO_2^- and ClO_3, which corresponds to 0.11 ± 0.00 and 0.17 ± 0.01 mg·g^{-1} of ClO_2^- and ClO_3, respectively (Fig. 5). Besides, the accessible porosity of CPC@GAC1 was kept with a slight reduction after 4 cycles (S_{BET} = 780 *vs.* 666 m^2·g^{-1}; SI Fig. S13), probably related with a small fraction of non-desorbed oxyanions during the regeneration process. At this point, we understand that the direct comparison with other adsorbents under continuous flow system is complex, since many variables affect the adsorption process (*e.g.,* initial concentration of oxyanions, flow rate, column dimensions, and regression analysis). Finally, and in contrast to the previous reported studies, our pilot-scale CPC@GAC1 prototype operated under conditions simulating those normally used in DWTPs. The efficient removal under these real conditions makes this system highly promising for the removal of ClO_2^- and ClO_3^- from drinking water.

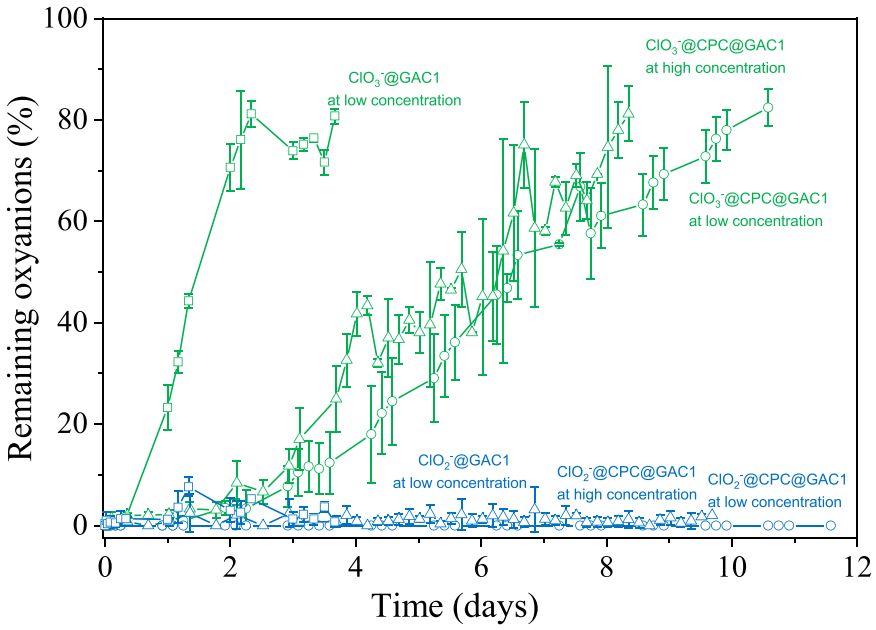

Fig. 4. Continuous flow removal of ClO_2^- (blue) and ClO_3^- (green) using the GAC1 (squares) in low concentration, and CPC@GAC1 at high (triangles) and low concentration (circles) with a water flow of 0.42 mL·min^{-1}, equivalent to *ca.* 0.12 m^3·h^{-1}m^{-2} and a bed contact time of 12 min. The Y-axis was estimated by remaining concentration in out-flow compared to concentration in-flow. (For interpretation of the references to color in this figure legend, the reader is referred to the web version of this article.)

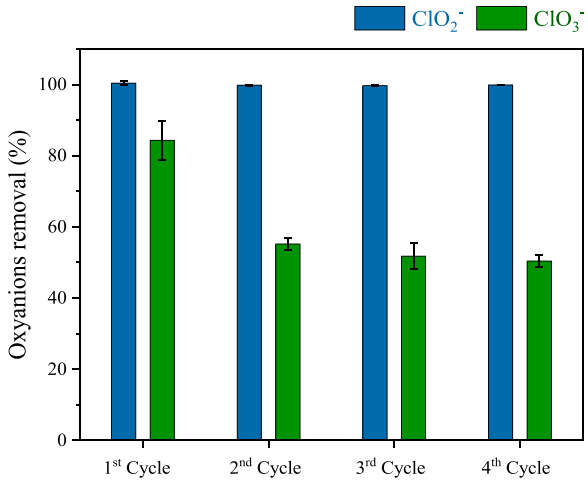

Fig. 5. Chlorite (blue bars) and chlorate (green bars) removal after 5.7 days in continuous flow for each cycle. (For interpretation of the references to color in this figure legend, the reader is referred to the web version of this article.)

4. Conclusions

The removal of disinfection by-products ClO_2^- and ClO_3^- from drinking water is a challenging process. The adsorbents' state-of-the art lacks from reasonable ClO_2^- and ClO_3^- removal capacities and/or show limited applicability in DWTPs. In this study, a simple and fast surface modification of the commercially-available granulated activated carbon GAC1 with the cationic surfactant hexadecylpyridinium chloride (CPC) increased its adsorption capacity between 2.2 to 2.4-fold. Further, a deep study of the process kinetics demonstrated the potential of CPC@GAC1 in continuous flow water treatment systems (with a complete removal of ClO_2^- and ClO_3^- in only 5 min). When tested under continuous flow compatible with real DWTPs, the time to reach 50% ($t_{50\%}$) of ClO_3^- saturation was 5.6-fold higher than the pristine GAC1. Finally, outstanding regeneration and reusability characteristics were shown with near quantitative removal and recovery rates after 4 consecutive adsorption and desorption cycles. All these results render CPC@GAC1 a promising adsorbent for drinking water purification, featuring rapid and effective removal of ClO_2^- and ClO_3^-. Overall, these results demonstrated that modified CPC@GAC1 shows outstanding performance for the treatment of drinking water. Work can be anticipated in extending these intriguing results to real implementation based on cost analysis and leaching evaluation. Finally, the cost production of 17.7 €·kg^{-1} was estimated for CPC@GAC1 material, but bulk material production is recommended to be optimized and exhaustive techno-economic feasibility for the next steps to be implemented in DWTPs.

CRediT authorship contribution statement

Rojas Sara: Conceptualization, Funding acquisition, Investigation, Methodology, Project administration, Resources, Supervision, Writing – original draft, Writing – review & editing. **Horcajada Patricia:** Conceptualization, Funding acquisition, Investigation, Methodology, Project administration, Resources, Supervision, Writing – original draft, Writing – review & editing. **Sanchez-Cano Gabriel:** Investigation, Methodology, Writing – original draft, Writing – review & editing. **Cristobal-Cueto Pablo:** Investigation, Methodology. **Nuño-Ortega Paula:** Investigation, Methodology. **Sáez Lydia:** Conceptualization, Funding acquisition, Investigation, Methodology, Project administration, Resources, Supervision, Writing – original draft, Writing – review & editing. **Lastra Antonio:** Conceptualization, Funding acquisition, Investigation, Methodology, Project administration, Resources, Supervision, Writing – original draft, Writing – review & editing.

Declaration of Competing Interest

The authors declare that they have no known competing financial interests or personal relationships that could have appeared to influence the work reported in this paper.

Data availability

Data will be made available on request.

Acknowledgements

This work has been supported by Canal de Isabel II Company and the IMDEA Energy Foundation through the Industrial Doctorate Project from the Community of Madrid (IND2019/AMB17129). S.R. is grateful for the grant (RYC2021-032522-I) funded by MCIN/AEI /10.13039/501100011033 and for El FSE invierte en tu future, and to the project CNS2022-135779 founded by MCIN/ AEI /10.13039/501100011033, B-FQM-394, and ProyExcel_00105 funded from Junta de Andalucía. G.S. thanks to S. Carrasco, T. Hidalgo, Y. Pérez-Cortés, C. Biglione, C. Fernández, G. Armani, I. Rincón, M. Abán for their experimental support and fruitful discussion. Funding for open access charge: Universidad de Granada / CBUA.

Appendix A. Supporting information

Supplementary data associated with this article can be found in the online version at doi:10.1016/j.jece.2024.112131.

References

[1] R.E. Cantwell, R. Hofmann, M.R. Templeton, J. Appl. Microbiol. 105 (2008) 25–35.
[2] S. Sorlini, M.C. Collivignarelli, M. Canato, J. Water Supply Res. Technol. AQUA 64 (2015) 450–461.
[3] M.C. Collivignarelli, A. Abbà, I. Benigna, S. Sorlini, V. Torretta, Sustainability 10 (2018) 1–21.
[4] W. Gan, H. Huang, X. Yang, Z. Peng, G. Chen, Environ. Sci. Water Res. Technol. 2 (2016) 838–847.
[5] N. Gonce, E.A. Voudrias, Water Res. 28 (1994) 1059–1069.
[6] EFSA Panel on Contaminants in the Food Chain, EFSA J. 13 (2015) 1–103.
[7] J. Wang, Y. Wu, L. Bu, S. Zhu, W. Zhang, S. Zhou, N. Gao, Water Res. 190 (2021) 116708.
[8] The European Parliament and the Council of the European Union, Off. J. Eur. Communities (2020) 35.
[9] P. Atkins, T. Overton, J. Rourke, M. Weller , F. Armstrong, Inorganic Chemistry, 2009.
[10] D. Couri, M.S. Abdel-Rahaman, R.J. Bull, Environ. Health Perspect. 46 (1982) 57–62.
[11] K. Alfredo, B. Stanford, J.A. Roberson, A. Eaton, J. Am. Water Works Assoc. 107 (2015) E187–E196.
[12] CN106011928A, 2016.
[13] 870054, 1979, 1–8.
[14] G.S. Cassol, C. Shang, J. Li, L. Ling, X. Yang, R. Yin, J. Environ. Sci. 117 (2022) 119–128.
[15] I.C. Clark, R.A. Melnyk, A. Engelbrektson, J.D. Coates, MBio 4 (2013) 1–11.
[16] A.F.W.M. Wolterink, E. Schiltz, P.L. Hagedoorn, W.R. Hagen, S.W.M. Kengen, A.J. M. Stams, J. Bacteriol. 185 (2003) 3210–3213.
[17] O. Wang, J. Coates, Microorganisms 5 (2017) 76.
[18] F. Torres-Rojas, D. Muñoz, N. Tapia, C. Canales, I.T. Vargas, Bioresour. Technol. 315 (2020) 123818.
[19] E. Sikora, G. Muránszky, F. Kristály, B. Fiser, L. Farkas, B. Viskolcz, L. Vanyorek, Int. J. Mol. Sci. 23 (2022) 1–13.
[20] Y. Yu, X. Huang, R. Chen, L. Pan, B. Shi, Chemosphere 280 (2021) 130958.
[21] Y. Shao, J. Li, X. Fang, Z. Yang, Y. Qu, M. Yang, W. Tan, G. Li, H. Wang, Chemosphere 287 (2022) 132118.
[22] T.M. Mubita, J.E. Dykstra, P.M. Biesheuvel, A. van der Wal, S. Porada, Water Res. 164 (2019) 114885.
[23] E.A. Voudrias, L.M.J. Dielmann, V.L. Snoeyink, R.A. Larson, J.J. McCreary, A.S. C. Chen, Water Res. 17 (1983) 1107–1114.
[24] S. Sorlini, C. Collivignarelli, Desalination 176 (2005) 255–265.
[25] W. fang Chen, Z.Y. Zhang, Q. Li, H.Y. Wang, Chem. Eng. J. 203 (2012) 319–325.
[26] U.S. Rashid , A.N. Bezbaruah, Chemosphere, DOI:10.1016/j.chemosphere.2020.126639.
[27] J. Fito, H. Said, S. Feleke, A. Worku, Environ. Syst. Res. 8 (1) (2019) 10.
[28] C. Pongener, D. Kibami, K.S. Rao, R.L. Goswamee, D. Sinha, J. Water Chem. Technol. 39 (2017) 108–115.
[29] A.F.Y. Adou, V.S. Muhandiki, Y. Shimizu, S. Matsui, Water Sci. Technol. 43 (2001) 1–7.
[30] Y. Li, T. Xu, C. Cui, Y. Li, Desalin. Water Treat. 53 (2015) 1881–1887.
[31] D. Angyal, I. Fábián, M. Szabó, Inorg. Chem. 62 (2023) 5426–5434.
[32] H. Baribeau, M. Prévost, R. Desjardins, P. Lafrance, D.J. Gates, J. Am. Water Works Assoc. 94 (2016) 96–105.
[33] S.Y. Lin, W.F. Chen, M.T. Cheng, Q. Li, Colloids Surf. A Physicochem. Eng. Asp. 434 (2013) 236–242.
[34] Sharlau, Activated Carbon, Granulated. ⟨https://www.scharlab.com/productos-producto-catalogo-productos-detalle-articulo.php?c=40&sc=261&p=7154⟩. (Accessed 22 June 2023).
[35] Sigma-Aldrich, NORIT® RX3 EXTRA, ⟨https://www.sigmaaldrich.com/ES/es/product/aldrich/901934⟩. (Accessed 22 June 2023).
[36] V. Subramanian, W.A. Ducker, Langmuir 16 (2000) 4447–4454.
[37] R. Epsztein, E. Shaulsky, N. Dizge, D.M. Warsinger, M. Elimelech, Environ. Sci. Technol. 52 (2018) 4108–4116.
[38] V. Patel, N. Dharaiya, D. Ray, V.K. Aswal, P. Bahadur, Colloids Surf. A Physicochem. Eng. Asp. 455 (2014) 67–75.
[39] S. Chotiradsirikun, R. Guo, A.S. Bhalla, H. Manuspiya, J. Porous Mater. 28 (2021) 117–128.
[40] R. Atkin, V.S.J. Craig, E.J. Wanless, S. Biggs, Adv. Colloid Interface Sci. 103 (2003) 219–304.
[41] W. Guo, Z. Fu, Z. Zhang, H. Wang, S. Liu, W. Feng, X. Zhao, J.P. Giesy, Sci. Total Environ. 710 (2020) 136302.
[42] S.K. Mehta, S. Kumar, S. Chaudhary, K.K. Bhasin, Nanoscale Res. Lett. 4 (2009) 1197–1208.
[43] S. Rojas, A. Torres, V. Dato, F. Salles, D. Ávila, J. García-González, P. Horcajada, Faraday Discuss. 231 (2021) 356–370.
[44] A. Dandekar, R.T.K. Baker, M.A. Vannice, Carbon 36 (1998) 1821–1831.
[45] M. Ouzzine, A.J. Romero-Anaya, M.A. Lillo-Ródenas, A. Linares-Solano, Carbon 67 (2014) 104–118.
[46] Torres-Rojas, F., Tapia, N., Vega, M., Alvear, C., Pizarro, G., Past, P., Cort, S., Vega, A.S. DOI:10.1016/j.envres.2023.116450.
[47] S. Committee, C. S. Sccs, S. Ii, Scientific Committee on Consumer Safety Cetylpyridinium chloride - Submission II COLIPA n ° P97, 2015.
[48] P.E. Jackson, TrAC Trends Anal. Chem. 20 (2001) 320–329.
[49] Š. Cerjan Stefanović, T. Bolanča, L. Ćurković, J. Chromatogr. A 918 (2001) 325–334.
[50] L. Barron, P.N. Nesterenko, B. Paull, J. Chromatogr. A 1072 (2005) 207–215.
[51] W. Plazinski, W. Rudzinski, A. Plazinska, Adv. Colloid Interface Sci. 152 (2009) 2–13.
[52] Y. Tong, P.J. Mcnamara, B.K. Mayer, Environ. Sci. Water Res. Technol. (2019) 821–838.
[53] K.L. Tan, B.H. Hameed, J. Taiwan Inst. Chem. Eng. 74 (2017) 25–48.
[54] S. Mallakpour, V. Behranvand, F. Mallakpour, J. Environ. Chem. Eng. 9 (2021) 105170.
[55] Q. Hu, S. Pang, D. Wang, Sep. Purif. Rev. 51 (2022) 281–299.
[56] J. Yuan, S. Mortazavian, E. Passeport, R. Hofmann, Sci. Total Environ. 838 (2022) 156406.
[57] M. El Gamal, H.A. Mousa, M.H. El-Naas, R. Zacharia, S. Judd, Sep. Purif. Technol. 197 (2018) 345–359.